Phase composition reproportioning of the plasma dynamic synthesisproduct of the zinc-bismuth-oxygen system

A A Sivkov, A S Ivashutenko, I A Rakhmatullin, Yu L Shanenkova and A I Tsimmerman

National Research Tomsk Polytechnic University, 30 Lenin Ave., Tomsk, 634050, Russia

E-mail: sivkovAA@mail.ru

Abstract. This article shows the possibility of obtaining nanosized materials based on zinc oxide and bismuth oxide by plasma dynamic synthesis. The main research in the article is the results on the influence of the precursors mass on the products phase composition of the Zn-Bi-O system. X-ray phase analysis allowed to establish the possibility of zinc oxide and bismuth oxide synthesis in one short cycle of the coaxial magnetoplasma accelerator. Changing the metal bismuth batch weight allows to adjust the bismuth oxide content in the final product. Transmission electron microscopy confirms the presence of zinc oxide phases in the bismuth oxide shell in the obtained material. Evaluation of the bismuth oxide shell thickness by determining the average size of the coherent scattering region showed that it is 30 nm.

1. Introduction

Zinc oxide ZnO has a unique combination of semiconductor, luminescent, piezoelectric and ferroelectric properties. Due to the set of these properties, its scope is huge, for example, in metallurgy (for the manufacture of electric cables), dentistry (abrasive materials), medicine (antiseptic), electronic industry (varistors). ZnO is characterized by low cost, high chemical, thermal and radiation resistance, as well as environmental friendliness [1–3]. In the classical ZnO-based varistor, in addition to the main component, impurities from various metal oxides are used, for example, bismuth (III), antimony, yttrium, zirconium, cobalt, manganese, plumbum, aluminum oxides, etc. [4–6], the addition of which characterizes an exceptional nonlinearity of the current-voltage characteristics.

Currently, nanodispersed zinc oxide is obtained by various technologies, for example, thermal decomposition of acetate, the sol-gel method, chemical and hydrothermal synthesis [3, 7, 8]. However, all these methods have a number of drawbacks: the multi-stage process and the presence of hard-to-remove impurity compounds in the final product.

The paper shows the possibility of obtaining nanostructured ZnO by the plasma dynamic method, the main component of which is a coaxial magnetoplasma accelerator. The method is based on the high-velocity crystallization of the liquid phase under supersonic sputtering conditions [9, 10]. The wide distribution of varistors based on zinc oxide for surge protection involves the creation of a universal technique for obtaining a composite powder with an adjustable phase composition in a one-step process of their synthesis.

2. Experimental part

Experiments on the ultrafine product synthesis were carried out using the plasmadynamic method. This method is based on the use of the installation, the main element of which is a coaxial magnetoplasma accelerator (CMPA) (figure 1) [11–13]. The CMPA is powered from a capacitive energy storage device (table 1 «*C*») with a charging voltage U_{ch} up to 5 kV, a capacity C up to 28.8 mF and an accumulated energy W_c up to 360 kJ. To create a composite product of the zinc-bismuth-oxygen system, the working electrode is made of zinc (2). In this case, the metal bismuth Bi (manufacturer «Component reactive», Russia) powder is preliminarily laid in the plasma formation zone (a purity of about 99 % and an average particle size of about 100 μm). The reactor chamber is filled with oxygen under pressure of up to 1 atmosphere.

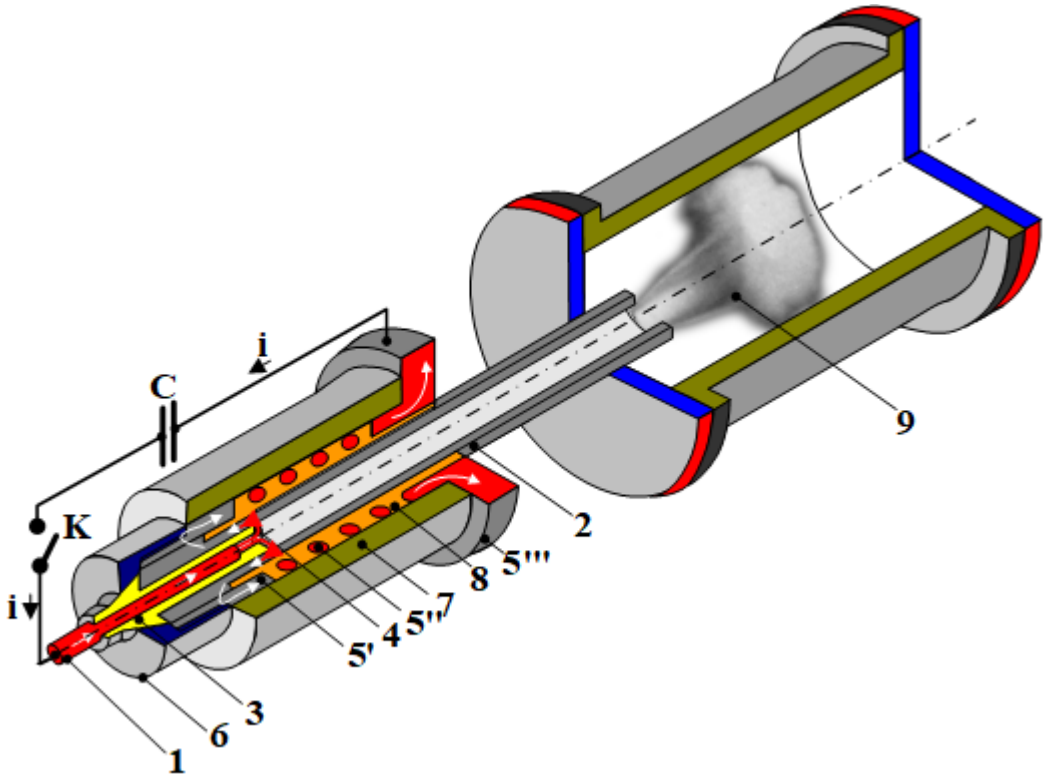

Figure 1. The scheme of the coaxial magnetoplasma accelerator:1 – central electrode, 2 – electrode-barrel, 3 – central electrode insulator, 4 – Z-pinch, 5 – inductor (5' – contact cylinder, 5" – solenoid, 5"' – contact flange), 6 – cap, 7 – case, 8 – insulation, 9 – plasma structure, I_m – maximum discharge current, U_m – voltage at maximum discharge current, W – energy input; m_{Bi}– the mass of the metal bismuth Bi deposited in the plasma formation zone; Δm_{er} – the mass of material electroerosive wear of the accelerating channel; m_p – the mass of synthesis plasma dynamic product.

Table 1. Basic parameters of the experiments.

№	U_{ch} (kV)	C (mF)	W_c (kJ)	I_m (kA)	U_m (kV)	W (kJ)	m_{Bi} (g)	Δm_{er} (g)	m_p (g)
1	3.4	4.8	27.7	109	1.1	10.1	1.25	13.2	9.01
2	3.4	4.8	27.7	148	1.1	20.5	2.50	19.5	9.86

The capacitive energy storage was charged to $U_{ch} = 3.4$ kV at $C = 4.8$ mF for an experiment to obtain a product based on zinc-bismuth-oxygen. In the considered experiments series, taking into account the data on the average mass erosion performance of zinc electrodes Δm_{er}, with marked

energy parameters, the mass of the metal bismuth Bi was equal to m_{Bi} = 1.25 g (experiment no. 1) and m_{Bi} = 2.50 g (experiment no. 2). These m_{Bi} values were chosen from considerations of obtaining the final mass percentage of $ZnO:Bi_2O_3$ approximately equal to 95.0%:5.0% and 90.0%:10.0%, respectively.

Figure 2 shows the oscillograms with the energy parameters presented above with different mass of the pledged material into the channel of formation of the plasma structure. When the keys K (figure 1) are closed, that is, the power supply to the accelerator electrodes (t = 0 μs), an aperiodic current begins to flow through the circuit, and when the current reaches a certain level, an electro-explosive destruction of the jumper wire occurs. In these experiments, the role of a conductive jumper is provided by bismuth and a graphite conductive layer sprayed from above, which provides a more reliable electrical contact between the electrodes. Thus, an arc plasma electric discharge is formed that captures bismuth (the first precursor). The arc electric discharge is accelerated in the acceleration channel and is compressed under the action of its own magnetic field and the magnetic field of the external inductor. As the plasma structure passes through the acceleration channel, an electroerosive accumulation of zinc material from the surface of the trunk occurs, which is captured by the plasma and passes into the plasma state. The formed plasma jet containing zinc and bismuth is taken out of the accelerating channel at a speed of about 4 km·s^{-1} [10] into the space of the working chamber-reactor, where the plasma-chemical reaction between zinc, bismuth and oxygen occurs when the material is sprayed from the plasma jet boundary. The oscillograms show that the process is about 500 μs. At the same time, in the experiment with a smaller mass of bismuth injected (experiment 1, figure 2a), the value of the summed energy W is about 10 kJ, which is almost two times less than in experiment no. 2 (figure 2b) W = 20.5 kJ. Such differences in energy values are due to the fact that in the first case, the intensity of electric blasting destruction of the jumper decreases due to less m_{Bi}. It is also worth noting that the mass of synthesis plasma dynamic powder m_p in the first case was about 6 g, and in the second it increased to 9 g due to an increase in the amount of supplied energy.

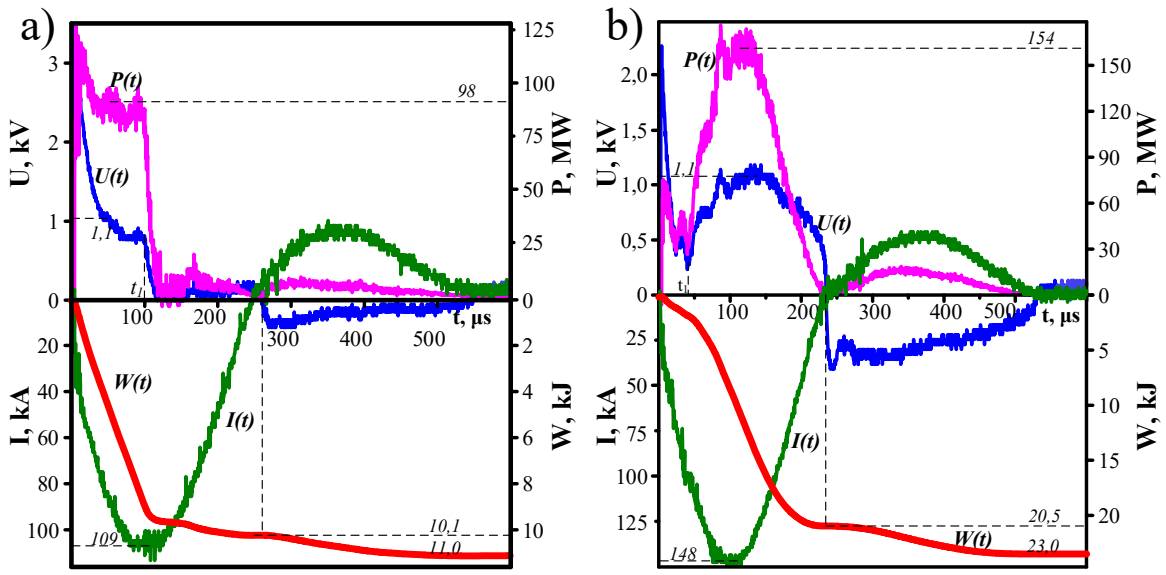

Figure 2. Typical oscillograms of the current of the power supply I(t), voltage at the accelerator electrodes $U(t)$, curves of the discharge power in the accelerating channel $P(t)$ and the input energy. a) №1; b) №2.

The synthesized product by the plasmodynamic method without additional thermal or other treatments was studied by X-ray diffractometry (Shimadzu XRD 7000S) with a copper cathode (CuK α_1 radiation, λ_1 = 1.540598 Å). X-ray structural-phase analysis was performed using PowderCell 2.4 software and the PDF4+ structural data base. Particle size and morphology were investigated using

scanning electron microscopy (Hitachi TM3000) and transmission electron microscopy (Phillips CM12).

3. Results and discussion

The collection of the synthesized product was carried out after its complete precipitation on the walls of the reactor chamber (after about half an hour). Figure 3 shows the X-ray diffraction patterns of the synthesized materials for two experiments, differing in the mass of bismuth m_{Bi} in the plasma formation zone. In addition, structural models of the presumably formed zinc oxide materials ZnO and bismuth oxide Bi_2O_3 are presented. The table 2 shows the structural-phase analysis of the materials obtained.

It was established that in both cases considered, the main crystalline phase is zinc oxide ZnO, which is closest to the structural model of PDF: 00-036-1451 hexagonal syngony with the space group (SG): P63mc and density $\rho_x = 5.656$ g·cm^{-3}. In addition, the bismuth oxide Bi_2O_3 phase is closest to the tetragonal structural model PDF: 73-6885 with the SG: P-42/c and density $\rho_x = 9.166$ g·cm^{-3} in the XRD-pictures.

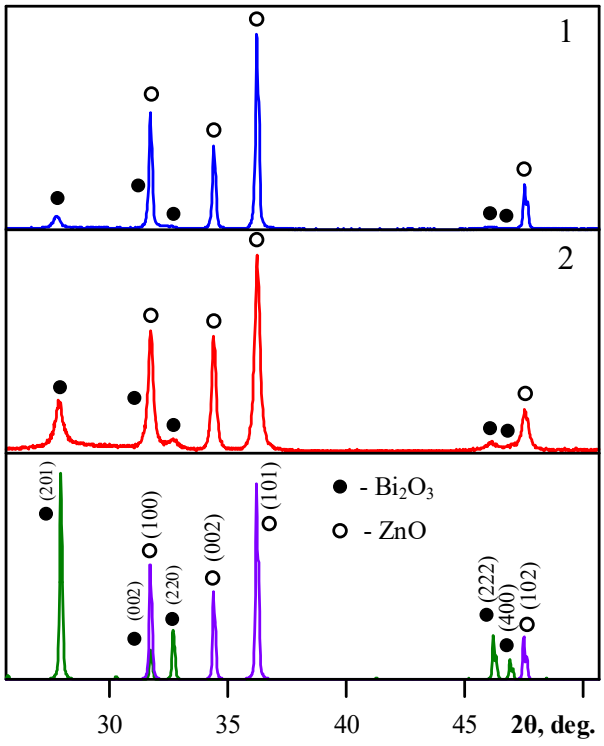

Figure 3. Diffractograms of the obtained powdery products of plasmodynamic synthesis with material cards from the PDF4+ database.

Table 2. Crystal lattice parameters.

Crystalline phase			ZnO	Bi_2O_3	Crystalline phase			ZnO	Bi_2O_3
Experiment 1					Experiment 2				
Phase content (wt. %)			95.3	4.7	Phase content (wt. %)			91.2	8.8
CSR (nm)			184	43	CSR (nm)			161	60
$\Delta d/d \cdot 10^{-3}$			0.35	2.50	$\Delta d/d \cdot 10^{-3}$			0.26	5.20
Lattice parameters (Å)	a	calculated	3.2493	7.7857	Lattice parameters (Å)	a	calculated	3.2321	7.6845
		reference	3.2498	7.7410			reference	3.2498	7.7410
	c	calculated	5.2033	5.6450		c	calculated	5.1781	5.6114
		reference	5.2066	5.6340			reference	5.2066	5.6340
Crystallinity (%)			71					76	

It can be seen from the table in figure 3 that in the first case, the content of crystalline ZnO is about ~ 95.3% with an average size of 184 nm coherent scattering regions (CSR) and the degree of internal microdistortion of the structure $\Delta d/d = 3.5\times10^{-4}$, while Bi_2O_3 is respectively around 4.7% with an average CSR size of ~ 43 nm and $\Delta d/d = 2.5\times10^{-3}$. In the second case, as expected, there is an increase in the bismuth oxide content to 8.8% due to an increase in the mass of the deposited metallic bismuth to 2.5 g and a corresponding increase in the energy of the process and the temperature of the plasma jet. The percentage of the main phase of ZnO decreases to 91.2% with a regular increase in CSR to 161 nm and $\Delta d/d = 2.6\times10^{-4}$. In this case, a noticeable increase in $\Delta d/d$ to 5.2×10^{-3} phases of bismuth oxide can be noted. In addition, I would like to note that the main advantage of the plasmodynamic method is the absence of residual phases of pure metals bismuth and zinc in the product synthesized.

The SEM images in figure 4 show that the powder in both cases is strongly agglomerated (figure 4, the first column is a resolution of ×200). In addition, shapeless specs of micron sizes are present in the product. It is formed from zinc oxide particles having a relatively low density of $\rho_{ZnO} = 5.61$ g·cm^{-3} and distinguished by a dark contrast, consolidated in a matrix of bismuth oxide, with a density of $\rho_{Bi2O3} = 9.16$ g·cm^{-3} and distinguished by a bright contrast on the SEM image. ZnO particles have a rounded shape and sizes less than 1.0 microns. The specs are formed due to the lower melting point of Bi_2O_3 ($T_m \approx 825$°C), which remains in the liquid phase for a long time, wets the already formed ZnO crystals ($T_p \approx 1975$°C) to compost the material and obtain zinc oxide ceramics with Bi_2O_3 and other additives components. The small fraction of the product with the minimum amount of specs and their minimum sizes, as shown in figure 4 with resolution ×30k (a) and ×10k (b), can be isolated both by traditional methods and directly during the synthesis by the method of buffer separation. It has a rather wide size distribution, including individual particles with a size of about 1 μm and a multitude of particles of the submicron and nanometer size ranges. A comparison of the SEM images of the previously synthesized pure ZnO material [10] and the material of the Zn-Bi-O system synthesized in this work shows the difference in the shapes of most particles. The particles obtained under the considered conditions have not geometrically and crystalline regular forms of single crystals, but round, but not spherical outlines. Taking into account the established phase composition of the products, it can be assumed that the particles of the composite powder are ZnO crystals in a bismuth oxide shell, which gives the particle a round shape.

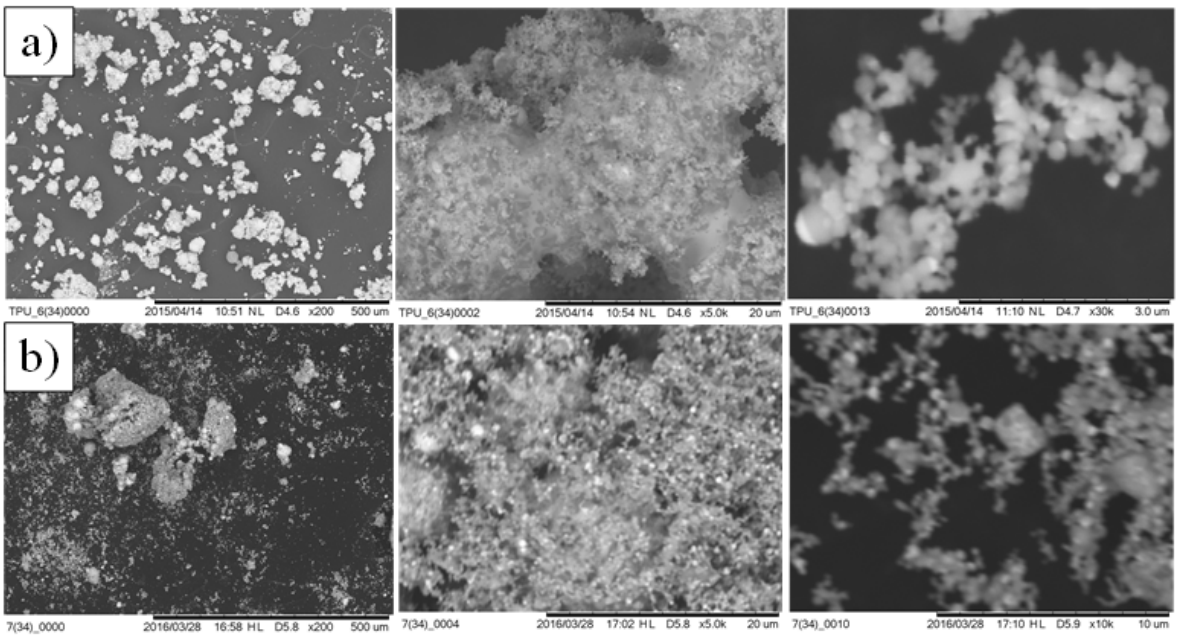

Figure 4. SEM-images for experiments a) no. 1; b) no. 2.

Transmission electron microscopy gives a clearer picture of the structure and morphology of the synthesized materials. Figure 5 shows the results of transmission microscopy in the form of bright field, dark field images of clusters of particles and electron microdiffraction patterns in a selected area in the light of the diffracted beams of two experiments, differing in different mass of metallic powder Bi. First of all, it should be noted that due to the greater value of the energy supplied by the accelerator in the second case (figure 5b), there is an increase in the particle size compared to the particle size in the experiment 1 (a).

In [10], a unique feature of the plasmodynamic synthesis method is shown, which consists in the fact that particles of a highly dispersed powder fraction with a size range from about 10 nm to 100 nm are hexagonal syngony single crystals with the classical growth form in the form of short hexagonal rods. On a typical bright field image of a composite product obtained in experiment 1 (figure 5a) with a smaller pad of metallic Bi, it is clear that the particles have a rounded shape in contrast to the particles of the synthesized zinc oxide material without additives. In light-field photographs of clusters of particles of composite products in the two experiments performed, the rounded particles are distinguished by a higher light density by the electron beam, and in the corresponding microelectronic diffraction only single point reflexes are seen. This is due to the significantly higher integral density of particles due to the presence of a shell of high-density bismuth oxide Bi_2O_3 on them.

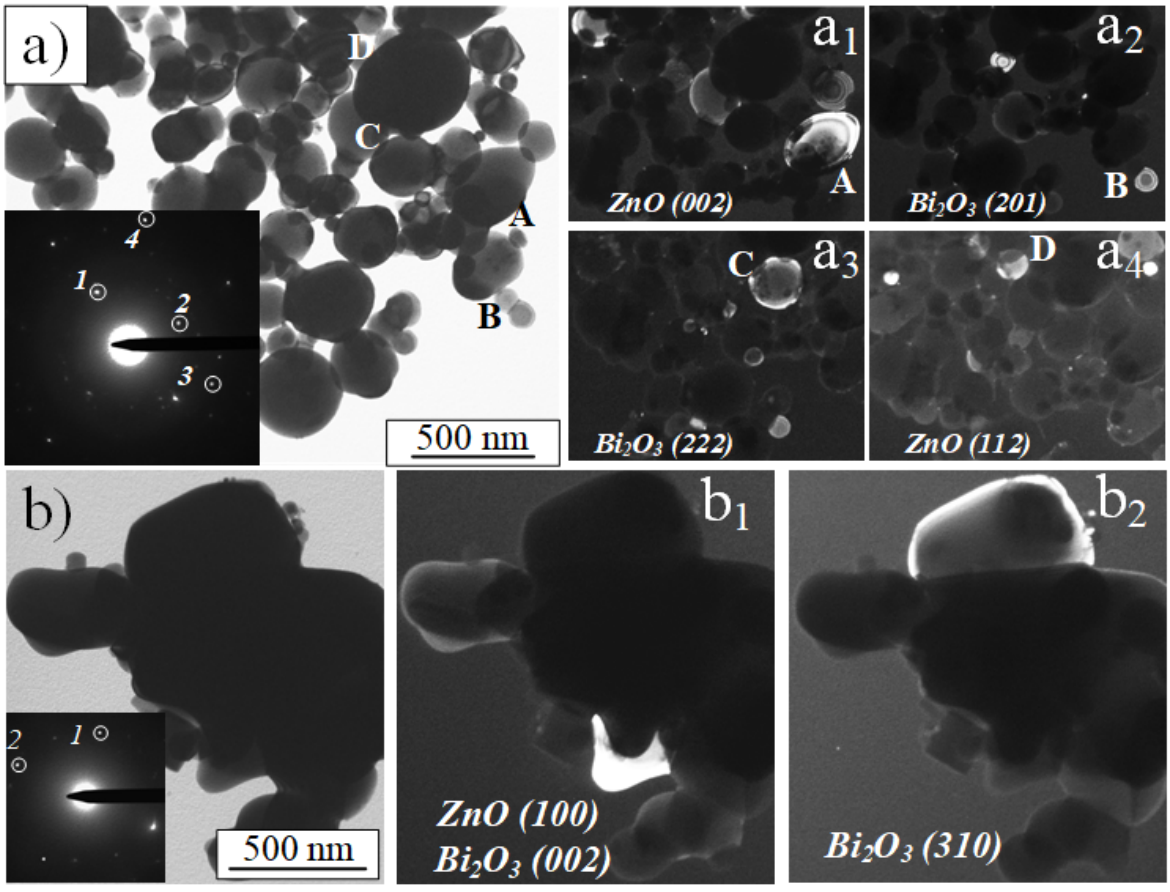

Figure 5. TEM-images for experiments a) no. 1; b) no. 2.

The captured dark-field images from the selected points on SAED clearly give an idea of the structure and phase composition of individual particles of the synthesized product. Reflexes 1 and 4, marked on SAED for the accumulation of particles of experiment 1 (a) and the corresponding dark-field images (a_1) and (a_4) exclusively contain the hexagonal structure of the zinc oxide phase in the [002] and [112] directions, respectively, and almost entirely luminous areas of rounded particles are

visible. While reflexes 2 and 3 (dark field images a_2 and a_3) are identified only by the Bi_2O_3 phase with a tetragonal structure in the [201] and [222] directions. For the second experiment, reflex 2 also corresponds only to the phase of bismuth oxide in the [310] direction. For these reflections, luminous diffraction contours are observed on the packages of planes of the crystalline Bi_2O_3 shell of rounded particles about 100 nm in size, as well as the glow of the peripheral zone of a large particle (about 200 nm) and the glow of particles of about 10 nm in size having a Bi_2O_3 shell. The marked reflex 1 in the cluster of the product of plasmodynamic synthesis obtained in experiment 2 (figure 5b) and the corresponding dark field image b_1 is determined by the phases of both zinc oxide [002] and bismuth oxide [100]. Apparently, the package of the [002] planes of the ZnO crystallite inside this particle is in the reflecting position of the Wulf-Bragg relative to the main electron beam and the beam diffracted on it illuminates the ellipsoid shell of bismuth oxide.

4. Conclusion

The paper shows the possibility of synthesizing a composite powder of a zinc-bismuth-oxygen system using a high-voltage high-current coaxial magnetoplasma erosion-type accelerator with a zinc accelerator channel. The results of X-ray structural analysis showed the possibility of obtaining by a plasma-dynamic method a composite dispersed material of composition $ZnO+Bi_2O_3$ without admixture of metal phases, the mass ratio of crystalline oxide phases in which can be adjusted by changing the mass of bismuth and energy of the synthesis process.

In addition, using transmission electron microscopy, it was confirmed that the particles contain two crystalline phases ZnO and Bi_2O_3. These data, together with the observed characteristic rounded shape of all particles in a powder with a known phase composition, according to XRD, once again confirm the assumption about the structure of particles as ZnO crystallites in a shell of crystalline bismuth oxide $Bi_2O_3$with a defective structure. The thickness of the shell can be estimated from the average size of the CSR phase of Bi_2O_3, which does not exceed 30 nm, while the average particle size in the powder is almost an order of magnitude higher.

Acknowledgments

The research was carried out at Tomsk Polytechnic University within the framework of Tomsk Polytechnic University Competitiveness Enhancement Program grant. The investigations on the synthesis of $ZnO-Bi_2O_3$ composite and corresponding improvement of the setup for plasma dynamic synthesis were funded by the Russian Foundation for Basic Research, grant No. 18-32-00115.

References

[1] Zhao S, Zhang Y, Zhou Y, Zhang C, Sheng X, Fang J and Yang Y 2017 *Appl. Surf. Sci.* **400** 269
[2] Li Y, Liu X, Chen X, Wang D and He Y 2017 *J. Alloys Compd.* **699** 468
[3] Gu H, Yu L, Wang J, Yao J and Chen F 2017 *Mater. Lett.* **196** 168
[4] Xiao X, Zheng L, Cheng L, Tian T, Ruan X and Li G 2015 *Ceram. Int.* **41** 557
[5] Bai H, Li S, Zhao Y, Xu Z, Chu R, Hao Jand Li G 2016 *Ceram. Int.* **42** 10547
[6] Xu Z, Bai H, Ma S, Chu R, Hao J, Chen C and Li G 2016 *Ceram. Int.* **42** 14350
[7] Cao J, Gong Y, Wang Y, Zhang B, Zhang H, Sun G and Zhang Z 2017 *Mater. Lett.* **198** 76
[8] Deshmukh P R, Sohn Y and Shin W G 2017 *J. Alloys Compd.* **711** 573
[9] Kuzenov V V, Polozova T N and Ryzhkov S V 2015 *Probl. Atomic Science Technology* **4** 49
[10] Sivkov A, Ivashutenko A, Shanenkova Y and Shanenkov I 2016 *Adv. Powder Technol.* **27** 1506
[11] Sivkov A A, Pak A Y, Nikitin D S, Rakhmatullin I A and Shanenkov I I 2013 *Nanotechnologies in Russia* **8** 489
[12] Shanenkov I I, Pak A Y, Sivkov A A and Shanenkova Y L 2014 *MATEC Web Conf.* **19** 01030
[13] Sivkov A, Saygash A, Kolganova J and Shanenkov I 2014 *IOP Conference Series: Mater. Sci. Eng.* **66** 012048